CrystEngComm

Accepted Manuscript

Structural Diversity of a series of coordination polymers built from 5-substituted isophthalic acid with or without methyl-functionalized N-donor ligand

De-Yun Ma,[1,†] Liang Qin,[1,†] Jia-Mei Lei,[†,‡] Yun-Qiu Liang,[†] Wei-Jie Lin,[†] Jing-Jing Yan,[†] Wan-Qiu Ding,[†] Hai-Fu Guo,[,†] and Yun Ling [*,§]*

[†]School of Chemistry and Chemical Engineering, Zhaoqing University, Zhaoqing 526061, P. R. China. Fax: +86-758-2752-796; Tel: +86-758-2752-796; E-mail: guohaifu@zqu.edu.cn

[‡] Chemical Engineering College of Inner Mongolia University of Technology, Hohhot 010051, China.

[§] Department of Chemistry, Fudan University, Shanghai, 200433, P. R. China. E-mail: yunling@fudan.edu.cn

[1] These authors contributed equally to this work.

ABSTRACT: The reaction of X-H_2BDC (X = H, Br, NO_2 and CH_3) and methyl-functionalized dmbpy ligands with metal salts under different solvent media conditions generate nine structural diversity zinc(II)/cadmium(II)-based coordination polymers (CPs), $\{[Zn_2(BDC)_2(DMF)_3]\cdot DMF\}_n$ (**1**), $[Zn(BDC)_2(dmbpy)]_n$ (**2**) $\{[(Me_2NH_2)_2Zn_3(Br\text{-}BDC)_4]\cdot 3DMF\cdot 3H_2O\}_n$ (**3**), $[Zn_2(Br\text{-}BDC)_2(dmbpy)]_n$ (**4**), $\{[Zn_{13}(NO_2\text{-}BDC)_8(\mu_3\text{-}OH)_2(\mu_2\text{-}OH)_6(H_2O)_4]\cdot 12H_2O\cdot 2NO_3\}_n$ (**5**), $[Zn_2(NO_2\text{-}BDC)_2(dmbpy)(H_2O)_2]_n$ (**6**), $\{[Cd(NO_2\text{-}BDC)(dmbpy)_{0.5}(H_2O)]\cdot(ACN)\cdot H_2O\}_n$ (**7**), $[Zn(CH_3\text{-}BDC)(dmbpy)_{0.5}(H_2O)]_n$ (**8**), and $[Zn(CH_3\text{-}BDC)(dmbpy)_{0.5}]_n$ (**9**) (H_2BDC = isophthalic acid, Br-H_2BDC = 5-bromoisophthalic acid, NO_2-H_2BDC = 5-nitroisophthalic acid, CH_3-H_2BDC = 5-methylisophthalic acid, dmbpy = 2,2′-dimethyl-4,4′-bipyridine, DMF = N,N-dimethylformamide, ACN = acetonitrile). All the compounds are synthesized using dual linkers (X-H_2BDC and dmbpy). **1** and **7-8** show 2D (4,4) network when dinuclear metal ions and ligands are regarded as nodes and linkers, respectively. **2** is a wave-like chain with the BDC ligands point alternately up and down. CPs **3-6** and **9** all exhibit 3D networks with 5-connected **sqp**, 6-connected **jsm**, 6-connected **pcu**, (3,4)-connected **dmc** and 6-connected **jsm** topologies, respectively. Furthermore, luminescent properties, thermo-gravimetric and chemical stability properties of these CPs were investigated. The results suggest that both organic ligands and solvent media influence on the final resulting CPs.

KEYWORDS: Coordination Polymers, Structural Diversity, 5-substituted isophthalate, Methyl-functionalized, Luminescence

Introduction

Metal-organic coordination polymers (CPs), as a relatively new type of inorganic-organic hybrid materials, have received widespread attention over the past decade owing to their modular assembly, structural diversity, fascinating topology, chemical tailorability and tenability, as well as their excellent properties with promising applications such as gas storage and separation, nonlinear optics, catalysis, magnetism, luminescence, drug delivery, sensing, and detection.[1] During the attainment of CPs, many factors can influence the construction progress, *e.g.*, metal ions, organic ligands, solvents, pH values, reaction temperatures, and so on.[2] Among many on-going efforts to develop high-performance CPs materials, selection and utilization of different organic ligands and solvent media are considered to be the two most significant factors that affect the structures and properties of final products.[3]

Moreover, a number of reports have shown that many carboxylate-based CPs involving transition metal ions (*e.g.* Zn^{2+}, Cd^{2+}, Co^{2+}) with or without the nitrogen-containing auxiliary ligands are unstable and lose their structural integrity rapidly when exposed to air due to the relatively weak metal-oxygen bonds within the frameworks are easy to be attacked by water molecules.[4] This drawback has been recognized as an imperative issue for their practical applications. Four main strategies are used to prepare the hydrophobicity carboxylate-based CPs: (1) using high oxidation state metals (*e.g.* Zr^{4+}, Cr^{3+}, *etc.*);[5a] (2) introducing the hydrophobic groups (*e.g.* methyl, ethyl) to the organic ligands;[4a] (3) doping hybrid composites (*e.g.* the carbon nanotubes or hetero-metals) into the frameworks to prepared the complex;[5b] (4)

using interpenetration or catenation of the frameworks to narrow the pore size.[5c] To our knowledge, very few examples of CPs based on carboxylate and dmbpy ligands have been reported.[3b,4a,6]

As part of an on-going study related to methyl-functionalized hydrophobicity CPs, the reactions of 5-substituted isophthalic acid (X-H_2BDC, X = H, Br, NO_2 and CH_3), 2,2′-dimethyl-4,4′-bipyridine (dmbpy) and metal salts under different solvent media conditions obtain nine new CPs with or without the N-donor ligands. Their structural diversities reveal that the solvent media and organic ligands play important role in the self-assembly processes. These nine CPs are characterized by elemental analyses, IR spectroscopy, thermogravimetric analyses, powder X-ray diffraction and single-crystal X-ray crystallography. The luminescent properties and the pH-dependent stabilities in aqueous solutions of **1-9** were investigated.

Experimental Section

Materials and methods

Materials and characterization. Reagent grade 5-substituted isophthalic acid (X-H_2BDC, X = H, Br, NO_2 and CH_3), $Zn(NO_3)_2{\cdot}6H_2O$ and $Cd(NO_3)_2{\cdot}4H_2O$ metal salts were obtained from Aladdin and used as received. 2,2′-dimethyl-4,4′-bipyridine (dmbpy) was isolated based on the reported procedures.[4a] Elemental analyses were carried out with a Vario EL III Elemental Analyzer. Infrared spectra were taken on a Shimadzu IR-440 spectrometer with a KBr disk in the 4000-400 cm^{-1} region. Thermogravimetric analyses (TGA) were carried out on an automatic simultaneous thermal analyzer (DTG-60, Shimadzu) under N_2 atmosphere at a heating rate of

10 °C/min within a temperature range of 25-800 °C. Powder X-ray diffraction patterns (PXRD) were collected using a Bruker AXS D8-Advance diffractometer with Cu-Kα (λ = 1.5418 Å) radiation. Luminescence spectra for crystalline samples were recorded at room temperature on an Edinburgh FLS920 phosphorimeter.

Syntheses of CPs 1-9

Synthesis of $\{[Zn_2(BDC)_2(DMF)_3]\cdot DMF\}_n$ (1). A mixture of $Zn(NO_3)_2\cdot 6H_2O$ (0.089 g, 0.3 mmol), H_2BDC (0.073 g, 0.3 mmol), and dmbpy (0.028 g, 0.15 mmol) was dissolved in 10 mL of DMF and stirred for 30 min. Then the solution was heated to 130 °C for 3 days in a 23 mL Teflon-lined stainless steel autoclave, followed by cooling to room temperature at 5 °C/h to yield colorless single crystals of **1** (yield: 40%, based on H_2BDC). Anal. calcd for $C_{28}H_{36}N_4O_{12}Zn_2$: C, 44.72; H, 4.79; N, 7.45. Found: C, 44.59; H, 4.96; N, 7.35. IR (KBr, cm^{-1}): 1604 (vs), 1557(s), 1478(m), 1445(w), 1356(vs), 1314(w), 1271(w), 1234(w), 1196(m), 1149(w), 1084(m), 1047(w), 939(w), 859(m), 836(m), 752(s), 717(s), 658(m), 588(m), 536(w), 451(w), 424(w) (see Figure S1 of the Supporting Information).

Synthesis of $[Zn(BDC)_2(dmbpy)]_n$ (2). The same synthetic procedure was followed to synthesized **2** as that **1** except solvent DMF was replaced by H_2O/EtOH (volume radio 1:1) (10 mL) (colorless crystals, yield: 55%, based on H_2BDC). Anal. calcd for $C_{28}H_{22}N_2O_8Zn$: C, 57.95; H, 3.79; N, 4.83. Found: C, 58.09; H, 3.66; N, 4.75. IR (KBr, cm^{-1}): 1637(m), 1576(vs), 1539(m), 1511(s), 1487(w), 1459(m), 1380(vs), 1271(m), 1215(w), 981(w), 779(w), 723(w), 672(w), 598(w), 554(w), 487(w), 435(w) (see Figure S1 of the Supporting Information).

Synthesis of {[$(Me_2NH_2)_2Zn_3(Br\text{-}BDC)_4$]·3DMF·3$H_2O$}$_n$ (3). The same synthetic procedure was followed to synthesized **3** as that **1** except H_2BDC was replaced by Br-H_2BDC (0.073 g, 0.3 mmol) (yellow crystals, yield: 32%, based on Br-H_2BDC). Anal. calcd for $C_{45}H_{54}N_5Br_4O_{22}Zn_3$: C, 35.37; H, 3.54; N, 4.58. Found: C, 35.29; H, 3.76; N, 4.35. IR (KBr, cm^{-1}): 3432(s), 3025(w), 2923(w), 2029(s), 1625 (s), 1557(m), 1434(m), 1359(s), 1250(w), 1100(m), 1018(w), 902(w), 840(w), 779(s), 717(s), 662(w), 567(w), 451(w) (see Figure S1 of the Supporting Information).

Synthesis of [$Zn_2(Br\text{-}BDC)_2(dmbpy)$]$_n$ (4). The same synthetic procedure was followed to synthesized **4** as that **3** except solvent DMF was replaced by H_2O/EtOH (volume radio 1:1) (10 mL) (yellow crystals, yield: 32%, based on Br-H_2BDC). Anal. calcd for $C_{28}H_{18}Br_2N_2O_8Zn_2$: C, 41.95; H, 2.25; N, 3.50. Found: C, 42.10; H, 2.14; N, 3.72. IR (KBr, cm^{-1}): 3088(w), 2985(m), 2022(s), 1714 (s), 1646(m), 1612(m), 1557(m), 1448(m), 1379(m), 1257(s), 1154(m), 1093(m), 1025(s), 895(w), 827(m), 772(m), 724(m), 649(w), 567(w), 492(w), 451(w) (see Figure S1 of the Supporting Information).

Synthesis of {[$Zn_{13}(NO_2\text{-}BDC)_8(\mu_3\text{-}OH)_2(\mu_2\text{-}OH)_6(H_2O)_4$]·12$H_2O$·2$NO_3$}$_n$ (5). The same synthetic procedure was followed to synthesized **5** as that **4** except Br-H_2BDC was replaced by NO_2-H_2BDC (0.063g, 0.3 mmol) (colorless crystals, yield: 55%, based on NO_2-H_2BDC). Anal. calcd for $C_{64}H_{64}N_{10}O_{78}Zn_{13}$: C, 25.02; H, 2.08; N, 4.56. Found: C, 25.13; H, 1.94; N, 4.67. IR (KBr, cm^{-1}): 3456(s), 2029(m), 1619 (s), 1571(m), 1530(m), 1455(m), 1373(s), 1346(s), 1291(w), 1202(w), 1079(m), 1018(w), 922(m), 827(m), 779(m), 737(s), 649(m), 553(w), 432(w) (see Figure S1 of the

Supporting Information).

Synthesis of $[Zn_2(NO_2\text{-}BDC)_2(dmbpy)(H_2O)_2]_n$ (6). The same synthetic procedure was followed to synthesized **6** as that **5** except solvent H_2O/EtOH (volume radio 1:1) was replaced by H_2O (10 mL) (yellow crystals, yield: 58%, based on NO_2-H_2BDC). Anal. calcd for $C_{28}H_{22}N_4O_{14}Zn_2$: C, 43.68; H, 2.86; N, 7.28. Found: C, 43.55; H, 2.98; N, 7.42. IR (KBr, cm^{-1}): 3345(s), 3081(w), 2027(s), 1619 (s), 1557(s), 1523(s), 1462(w), 1427(w), 1339(s), 1202(w), 1086(w), 1018(w), 929(w), 867(w), 820(w), 785(w), 730(s), 655(w), 574(w), 430(w) (see Figure S1 of the Supporting Information).

Synthesis of $\{[Cd(NO_2\text{-}BDC)(dmbpy)_{0.5}(H_2O)]\cdot(ACN)\cdot H_2O\}_n$ (7). The same synthetic procedure was followed to synthesized **7** as that **5** except $Zn(NO_3)_2\cdot 6H_2O$ and solvent H_2O/EtOH (volume radio 1:1) was replaced by $Cd(NO_3)_2\cdot 4H_2O$ (0.092g, 0.3 mmol) and solvent of H_2O/ACN (volume radio 1:1), respectively (colorless crystals, yield: 67%, based on NO_2-H_2BDC). Anal. calcd for $C_{16}H_{16}N_3O_8Cd$: C, 39.13; H, 3.26; N, 8.56. Found: C, 39.25; H, 3.18; N, 8.72. IR (KBr, cm^{-1}): 3443(s), 2944(w), 1654 (s), 1560(w), 1508(w), 1436(s), 1398(s), 1173(w), 1107(w), 1012(w), 972(w), 950(w), 850(w), 808(w), 740(w), 669(m), 651(w), 532(w), 424(w) (see Figure S1 of the Supporting Information).

Synthesis of $[Zn(CH_3\text{-}BDC)(dmbpy)_{0.5}(H_2O)]_n$ (8). The same synthetic procedure was followed to synthesized **8** as that **4** except Br-H_2BDC was replaced by CH_3-H_2BDC (0.053g, 0.3 mmol) (colorless crystals, yield: 56%, based on CH_3-H_2BDC). Anal. calcd for $C_{15}H_{14}NO_5Zn$: C, 50.90; H, 3.96; N, 3.96. Found: C,

51.25; H, 3.68; N, 3.72. IR (KBr, cm^{-1}): 3441(s), 2921(w), 1703(s), 1637 (s), 1604(s), 1562(w), 1508(w), 1455(w), 1380(s), 1328(m), 1215(s), 1023(w), 929(w), 831(s), 779(s), 752(m), 719(s), 681(m), 643(m), 461(w) (see Figure S1 of the Supporting Information).

Synthesis of $[Zn(CH_3\text{-}BDC)(dmbpy)_{0.5}]_n$ (9). The same synthetic procedure was followed to synthesized **9** as that **8** except solvent H_2O/EtOH (volume radio 1:1) was replaced by H_2O (10 mL) (purple crystals, yield: 53%, based on CH_3-H_2BDC). Anal. calcd for $C_{15}H_{12}NO_4Zn$: C, 53.79; H, 3.59; N, 4.18. Found: C, 53.65; H, 3.52; N, 4.38. IR (KBr, cm^{-1}): 2977(w), 1628(vs), 1553(m), 1515(m), 1459(s), 1422(m), 1375(s), 1347(w), 1244(w), 1051(w), 831(w), 775(w), 719(m), 672(w), 419(w). (see Figure S1 of the Supporting Information).

X-ray Crystallography Measurements

Single crystal data for CPs **1-3, 5-9** and **4** were collected on a Bruker Apex II CCD diffractometer equipped at 50 kV and 30 mA with MoKα radiation (λ = 0.71073 Å) and CuKα radiation (λ = 1.54178 Å), respectively. Data collection and reduction were performed using the APEX II software.[7a] The structures were solved using direct methods followed by least-squares on F^2 using SHELXTL.[7b] Non-hydrogen atoms were refined with independent anisotropic displacement parameters and hydrogen atoms attached to carbon and oxygen were placed geometrically and refined using the riding model. The more detailed information is listed in the CIF file. Topological analyses of the compounds were performed by using the TOPOS software.[8] Crystallographic data and structural refinement detail of CPs **1-9** can be found in

Table 1. Selected bond lengths and bond angles are given in Table S1. H-bonding parameters for **2** and **6-8** are given in Table S2 (see the Supporting Information).

Results and discussion

Description of crystal structures

{[Zn_2(BDC)$_2$(DMF)$_3$]·DMF}$_n$ (1). Compound **1** has (4,4) layered structure, crystallizing in the monoclinic space group $P2_1$. The thermal ellipsoid plot of the asymmetric unit of **1** is shown in Fig. 1a. In the asymmetric unit of **1**, there are two crystallographically independent zinc ions (Zn1 and Zn2), two BCD anions, three DMF ligands and one free DMF molecule. Both Zn1 and Zn2 are six-coordinated by six carboxylate oxygen atoms from four different BDC ligands for Zn1, three carboxylate oxygen atoms from three BDC anions and three DMF ligands for Zn2, and displays the same octahedral coordination. The Zn-O bond lengths and O-Zn-O bond angles range from 2.045(8) Å to 2.314(7) Å and 57.3(3)° to 179.3(3)°, respectively, which is within the reasonable range of observed values for other six-coordinated Zn(II) complexes with oxygen donating ligangds.[9] In the crystal structure of **1**, the BDC ligands act as bridging μ_3 and μ_4 modes to link three and four zinc ions, respectively (Scheme 1: modes I-II). In this manner, the dinuclear zinc units are connected by μ_3-BDC ligands to generate a linear chain of [Zn_2(BDC)(DMF)$_3$]$_n$ with dinuclear zinc cores separated by 10.145 Å (Fig. 1b), in which the chains are further connected into a (4,4) layered structure through μ_4-BDC ligands when dinuclear zinc units and BDC ligands are regarded as nodes and linkers, respectively (Fig. 1c).

[Zn(BDC)$_2$(dmbpy)]$_n$ (2). Compound **2** crystallizes in the monoclinic space group *C2/c*, with one Zn atom, one BDC ligand and half a dmbpy ligand in the asymmetric unit. The four-coordinated Zn(II) center is surrounded by two oxygen atoms from two BDC ligands and two nitrogen atoms from two dmbpy ligand, which exhibits a distorted tetrahedral coordination geometry (Fig. 2a), with Zn-O, Zn-N distances of 1.9727(17) Å, 2.097(2) Å and O-Zn-O, O-Zn-N bond angles of 100.62(8)°, 108.75(7)° and 127.96(11)°, respectively, all of within the range of those found in other four-coordinated Zn(II) complexes with oxygen and nitrogen donating ligands.[10] In the polymeric structure of **2**, the BDC and dmbpy ligands act in monodentate terminal and bidentate bridging modes, respectively (Scheme 1: modes III and VIII). In this manner, the μ_2-dmbpy ligands link zinc centers to result in a wave-like chain with the BDC ligands point alternately up and down with respect to the chain (Fig. 2b). The Zn⋯Zn separation of the chain is 11.308 Å. The adjacent chains are bridged by inter/intramolecular hydrogen bonds (O-H⋯O and C-H⋯O) to form a 3D framework (Fig. 2c and 2d, Table S2).

{[(Me$_2$NH$_2$)$_2$Zn$_3$(Br-BDC)$_4$]·3DMF·3H$_2$O}$_n$ (3). Single-crystal X-ray diffraction measurement shows that CP **3** crystallizes in the *Pbca* space group, and the asymmetric unit of **3** contains three Zn^{II} atom, four Br-BDC anion, two charge-balancing $[Me_2NH_2]^+$ cations, three free DMF molecule and three lattice water molecules. The perspective representations of the trinuclear CP **3** is shown in Fig. 3a. The three zinc ions in **3** form an almost linear $[Zn_3(\mu_2\text{-OOC}_{bridging})_6(\mu\text{-OOC}_{monodentate})_2]$ unit with Zn1⋯Zn2 and Zn1⋯Zn3 distances of 3.666 Å and 3.701 Å, respectively.

Both Zn2 and Zn3 are four-coordinated by four carboxylate oxygen atoms from four different Br-BDC ligands, adopting the same distorted tetrahedral coordination sphere; Zn1 is six-coordinated by six carboxylate oxygen atoms from six different Br-BDC ligands and displays an octahedral coordination geometry. The Zn-O distances and O-Zn-O bond angles ranging from 1.942(4) Å to 2.112(4) Å and from 80.70(16)° to 175.93(17)°, respectively, all of which are within the range of those reported in other trinulcear zinc(II) compounds involving carboxylate ligands.[11,10c] In the crystal structure of **3**, the Br-BDC ligands act as bridging μ_3 and μ_4 modes to link three and four metal ions, respectively (Scheme 1: modes IV and V). In this manner, the trinuclear zinc clusters are connected by Br-BDC ligands to obtain a wave-like infinite chain of $[Zn_3(Br\text{-}BDC)_6]_n$ with trinuclear zinc cores separated by 9.096 Å and 11.025 Å, respectively (Fig. 3b), in which the chains are further linked into a layered structure through μ_3-Br-BDC ligands with rectangle meshes (Fig. 3c). Finally, the 2D layered network concatenates another 2D layer *via* carboxylate oxygen atoms to form an ideal 3D framework (Fig. 3d). Topologically, the trinuclear zinc clusters act as 5-connected nodes, and Br-BDC ligands as linkers. CP **3** represents 5-connected **sqp** net with a point symbol of $(4^4.6^6)$ (Fig. 3e). **3** represents a charged anionic MOF[12] with the charge-balancing $[Me_2NH_2]^+$ cations, DMF and water guest molecules in the pores. The $[Me_2NH_2]^+$ cation was generated by the decomposition of DMF under the solvothermal conditions.[12a]

$[Zn_2(Br\text{-}BDC)_2(dmbpy)]_n$ (4). CP **4** crystallizes in the orthorhombic space group $C222_1$ and exhibits a 3D framework constructed by dmbpy ligands and dinuclear

secondary-building units of $[Zn_2(Br\text{-}BDC)_4]_n$. The asymmetric unit of **4** includes four crystallographically independent Zn^{2+} ions, four Br-BDC anions and two dmbpy ligands. Each Zn(II) center is five-coordinated by four carboxylate oxygen atoms from four different Br-BDC ligands and one nitrogen atom from one dmbpy ligand (Fig. 4a), adopting a distorted trigonal bipyramidal geometry with Zn-O distances and O-Zn-O bond angles ranging from 1.964(13) Å to 2.104(14) Å and from 83.5(5)° to 164.2(5)°, respectively, all of which are within the reasonable range of those reported for other five-coordinated Zn(II) complexes with oxygen and nitrogen donating ligands.[13] In the polymeric structure of **2**, the Br-BDC ligands adopt the μ_4 bridging mode to connect four Zn(II) ions, whereas dmbpy ligand acts as a *trans* bidentate bridging mode to link two Zn(II) ions with dinuclear zinc cores separated by 14.022 Å, 14.012 Å and 14.057 Å, respectively (Scheme 1: modes V and VIII). The four Br-BDC ligands link two Zn^{II} ions to construct a dinuclear zinc building block, which can be regarded as a supramolecular secondary building unit (SBU) or knot. The connectivity of Br-BDC ligand leads to the formation of a zigzag-like infinite chain with the separations of 9.196 Å and 9.428 Å between two dinuclear zinc cores (Fig. 4b), in which the chains are further extended into a layered structure (Fig. 4c). The rigid μ_2-dmbpy struts point alternately up and down with respect to the layer (Fig. 4d), and link neighboring layers to result in an ideal three-dimensional structure (Fig. 4e). Topologically, each SBU can act as 6-connected node, Br-BDC and dmbpy ligands as linkers, and **4** can be represented as a **jsm** net with a point symbol of $(5^{10}.6^4.7)$ (Fig. 4f).

{[$Zn_{13}(NO_2$-BDC$)_8(\mu_3$-OH$)_2(\mu_2$-OH$)_6(H_2O)_4]\cdot 12H_2O\cdot 2NO_3\}_n$ (5). 5 crystallizes in the triclinic space group *P-1*, with six Zn^{2+} ions plus another on a crystallographic inversion center, four NO_2-BDC ligands, one μ_3-O atoms, three μ_2-O atoms, two aqua ligands, six lattice water molecules and one NO_3 anion in the asymmetric unit (Fig. 5a). **5** is a 3D framework consisting of [Zn_6O_{22}] hexanuclear and [Zn_7O_{24}] heptanuclear building blocks. The [Zn_6O_{22}] hexanuclear building block contains three crystallographically independent Zn(II) ions assuming different coordination environments, as shown in Fig. 5b. The distorted octahedral geometry of Zn2 are occupied by three caryboxylate oxygen atoms (O2, O7, O23) from three NO_2-BDC ligands, two μ_3-O atoms (O25, O25^i, symmetry code: i = -x, 2-y, -z) and one μ_2-O atom (O26) from the coordination hydroxyl groups. The distorted tetrahedral geometry of Zn1 is surrounded by three carboxylate oxygen atoms (O1, O14, O24) from three NO_2-BDC ligands, and one μ_3-O atom (O25) from the coordination hydroxyl group. The Zn3 ion is also four-coordination by two carboxylate oxygen atoms (O8, O13) from two NO_2-BDC ligands and two μ_2-O atoms (O26, O27) from two coordination hydroxyl groups. The Zn-O average bond distances of Zn1 (1.975 Å) and Zn3 (1.941 Å) are shorter than that of Zn2 (2.119 Å), which is consistent with the fact that the bond distances in a tetrahedral geometry are generally shorter than those in other geometries.[14] Three pairs of crystallographically equivalent Zn1, Zn2 and Zn3 ions are bridged by two μ_2-O atoms and two μ_3-O atoms to give a [Zn_6O_{22}] hexanuclear building block with shorter separations of Zn⋯Zn (Zn1⋯Zn2, 3.156 Å; Zn1⋯Zn3, 3.868 Å; Zn2⋯Zn3, 3.399 Å). For [Zn_7O_{24}] heptanuclear building blocks

(Fig. 5c), there are four crystallographically independent Zn(II) ions with square-planar geometry for Zn6, and distorted tetrahedral geometry for Zn4, Zn5 and Zn7. Zn6 is surrounded by two carboxylate oxygen atoms ($O10^{v}$, $O10^{vi}$, symmetry codes: v = 1+x, y, z; vi = -x, 2-y, 1-z) from two NO_2-BDC ligands and two μ_3-O atoms (O28, $O28^{vii}$, symmetry codes: vii = 1-x, 2-y, 1-z). All of Zn4, Zn5 and Zn7 are four-coordination by two carboxylate oxygen atoms (O17, O19), two μ_2-O atoms (O27, O28) for Zn4, three carboxylate oxygen atoms (O6, O18, O20), one aqua ligand (O1W) for Zn5, two carboxylate oxygen atoms (O5, O9), one μ_3-O atom (O28) and one aqua ligand (O2W) for Zn7. Four pairs of crystallographically equivalent Zn4, Zn5, Zn6 and Zn7 ions are linked by two μ_3-O atoms and carboxylate oxgyens to give a $[Zn_7O_{24}]$ heptanuclear building block with shorter separations of Zn···Zn (Zn4···Zn5, 3.106 Å; Zn4···Zn6, 3.110 Å; Zn4···Zn7, 3.543 Å; Zn5···Zn6, 3.699 Å; Zn5···Zn7, 3.600 Å; Zn6···Zn7, 3.385 Å). It is rare that the hexanuclear and heptanuclear building blocks with different coordination environments of metal center are in one compound. The two types of adjacent building blocks are connected to each other through a carboxylate group and a μ_2-O atom (O27), resulting in the formation of a 1D chain (Fig. 5d), which is extended into a 2D layered structure (Fig. 5e). The bridging of the neighboring Znic(II) clusters occurs in the four directions, which leads to formation of the 3D network (Fig. 5f). Topologically, both $[Zn_6O_{22}]$ hexanuclear and $[Zn_7O_{24}]$ heptanuclear building blocks can be regarded as 6-connected nodes, and **5** can be represented as a **pcu** net with a point symbol of $(4^{12}.6^3)$ (Fig. 5g).

$[Zn_2(NO_2\text{-}BDC)_2(dmbpy)(H_2O)_2]_n$ (6). **6** crystallizes in the monoclinic space

group $P2_1/c$, with one Zn^{2+} cation, one NO_2-BDC ligand, half a dmbpy ligand and an aqua ligand in the asymmetric unit. As shown in Fig. 6a, each Zn(II) center is five-coordinated by three carboxylate oxygen atoms from three NO_2-BDC ligands, one nitrogen atom from a dmbpy ligand, and an aqua ligand to give a distorted trigonal bipyramidal coordination geometry. The bond lengths surrounding the Zn(II) center (Zn-O and Zn-N bond distances) are in the range of 1.9652(11)-2.2260(12) Å, and the bond angles are in range of 83.03(4)-124.46(5)°. The values are in agreement with those found in other five-coordinated Zn(II) complexes with oxygen and nitrogen donating ligands.[13] In the crystal structure of **6**, the NO_2-BDC ligands act as a bridging μ_3 mode to link three metal ions, whereas the dmbpy ligand has a bridging μ_2 mode connecting two metal ions (Scheme 1: modes VI and VIII). In this manner, the zinc(II) ions are connected into a wave-like infinite chain with the Zn⋯Zn separations of 8.636 Å and 11.167 Å (Fig. 6b), which is extended into a 2D layer (Fig. 6c). The bridging of the neighboring zinc(II) ions occurs in the four directions, which leads to formation of the 3D framework (Fig. 6d). Moreover, O-H⋯O and C-H⋯O hydrogen bonds are also observed (Table S2). Topologically, the Zn^{II} centers and NO_2-BDC ligands act as 4-connected and 3-connected nodes, respectively, dmbpy ligands as linkers, and **6** can be represented as a **dmc** net with a point symbol of $(4.8^2)(4.8^5)$ (Fig. 6f).

$\{[Cd(NO_2\text{-}BDC)(dmbpy)_{0.5}(H_2O)]\cdot(ACN)\cdot H_2O\}_n$ (7). Single-crystal X-ray diffraction analysis reveals that **7** has a (4,4) layered structure, crystallizing in the triclinic space group *P-1*. In the asymmetric unit of **7**, there is one Cd(II) cation, one

NO_2-BDC anion, half a dmbpy ligand, one aqua ligand, one ACN molecule (acetonitrile) and one lattice water molecule. As shown in Fig. 7a, the Cd(II) centre is six-coordinated by four carboxylate oxygen atoms from three NO_2-BDC anions, one nitrogen atom from one dmbpy ligand and one aqua ligand, displaying a distorted pentagonal bipyramidal geometry. The Cd-O, Cd-N bond lengths and O-Cd-O, O-Cd-N, N-Cd-N bond angles, all within the ranges of those for seven-coordinated Cd(II) complexes with oxygen and nitrogen donating ligands,[15] are ranging from 2.299(2) Å to 2.646(2) Å and 52.20(7)° to 143.00(8)°, respectively. In the complicated structure, carboxyl of NO_2-BDC anions adopts one coordination fashion: uses a chelating-bridging mode and a monodentate mode to link three Cd(II) ions, whilst the dmbpy ligand serves as a *trans* bidentate bridging mode to link two Cd(II) ions (Scheme 1, modes VII and VIII). Every three NO_2-BDC anions coordinate to one Cd atom to produce a 1D double chain of $[Cd_2(NO_2\text{-BDC})_2]_n$ (Fig. 7b). It is worth noting that the $[Cd_2(NO_2\text{-BDC})_2]_n$ motif features a double-linear chain with a long pitch of about 10.066 Å. The double chain differs structurally from that reported previously,[16] where the carboxylate ligands with metal ions are almost coplanar. Adjacent chains are connected into a (4,4) layered network, if the dinuclear zinc metal ions are regarded as 4-connected node (Fig. 7c). Finally, the layers are further assembled into a 3D supramolecular structure through additional O-H⋯O hydrogen bonding interactions involving the carboxylate oxygen atoms NO_2-BDC ligands, aqua ligands, free water molecules and nitrogen atoms of acetonitrile molecule (Fig. 7d and 7e, Table S2). Moreover, intramolecular C13-H13⋯O2 hydrogen bonds are also

observed (Table S2).

[Zn(CH_3-BDC)(dmbpy)$_{0.5}$(H_2O)]$_n$ (8). Compound **8** also shows a (4,4) layered structure, crystallizing in the triclinic space group *P-1*, with one zinc cation, one CH_3-BDC anion, half a dmbpy ligand and one aqua ligand. As shown in Fig. 8a, each Zn(II) center is six-coordinated by four carboxylate oxygen atoms from three CH_3-BD anions, one nitrogen atom from a dmbpy ligand, and an aqua ligand to generate a distorted pentagonal bipyramidal geometry. The Zn-O, Zn-N bond distances and O-Zn-O, O-Zn-N bond angles are in the range of 2.309(6)-2.378(5) Å and 81.0(2)-170.58(18)°, respectively, which the values are in agreement with those found in other six-coordinated Zn(II) complexes with oxygen and nitrogen donating ligands.[17] In the crystal structure of **8**, the CH_3-BDC ligands act as bridging μ_3 mode to link three zinc ions (Scheme 1: modes I and VIII). In this manner, the dinuclear zinc units are connected by μ_3-CH_3-BDC ligands to obtain a linear chain of [Zn_2(CH_3-BDC)$_2$(dmbpy)$_2$(H_2O)$_2$]$_n$ with dinuclear zinc cores separated by 9.867 Å (Fig. 8b), in which the chains are further pillared by dmbpy struts into a 2D (4,4) network when dinuclear zinc units and organic ligands (CH_3-BDC and dmbpy) are regarded as nodes and linkers, respectively (Fig. 8c). These layers are finally connected into a 3D supramolecular structure through O-H⋯O hydrogen bonds involving the aqua ligands and carboxylate oxygen atoms (O1 and O4) (Fig. 8d and 8e, Table S2). Moreover, intramolecular C-H⋯O hydrogen bonds have also been observed (Table S2).

[Zn(CH_3-BDC)(dmbpy)$_{0.5}$]$_n$ (9). The crystal structure analysis reveals that compound

9 crystallizes in the tetragonal system with the space group *I4122* and exihibits a 3D coordination framework built from dinuclear zinc(II) units with μ_4-CH_3-BDC and μ_2-dmbpy ligands. The asymmetric unit consists of one Zn^{II} ion, half a CH_3-BDC anion and a quarter of dmbpy ligand. As shown in Fig. 9a, each zinc ions is penta-coordinated by one N atom from the dmbpy ligand, and four O atoms from four different CH_3-BDC anions, leaving a silghtly distorted square pyramid coordination geometry. The Zn-O, Zn-N bond distances and O-Zn-O, O-Zn-N bond angles ranging from 2.009(2) Å to 2.082(3) Å and 88.30(11)° to 167.70(17)°, respectively, all of which are within the range of those reported in other penta-coordinated Zn(II) complexes with oxygen and nitrogen donating ligangds.[13] In the complex **9**, each CH_3-BDC^{2-} ligand is completely deprotonated and act as bridging μ_4 mode to link four zinc ions, whereas the dmbpy ligand acts as a *trans* bidentate bridging mode to link two Zn(II) ions (Scheme 1: modes V and VIII). In this manner, the μ_4-CH_3-BDC ligands links dinuclear zinc units to result in a wave-like chain with dinuclear zinc cores separated by 9.323 Å (Fig. 9b), in which these chains are further connected into a 3D framework with rectangle meshes through other μ_4-CH_3-BDC^{2-} anions and μ_2-dmbpy ligands (Fig. 9c). Topologically, the dinuclear zinc units and organic (CH_3-BDC and dmbpy) ligands act as 5-connected nodes and linkers, and **9** can be represented as a **jsm** net with a point symbol of $(5^{10};6^4;7)$ (Fig. 9d).

The synthesis and structural comparison of 1-9

By changing the solvent media, nine new zinc/cadmium-based CPs are synthesized based on the reaction of V-shaped linker molecule of substituted 1,3-benzene

dicarboxylic acid, X-H_2BDC (X = H, Br, NO_2 and CH_3) and the methyl-functionalized ligand (dmbpy) under the same reaction temperature (130 °C). All the CPs, described in this article, are synthesized using dual linkers and these dual linkers are chosen as following: (H_2BDC, dmbpy) for CPs **1-2,** (Br-H_2BDC, dmbpy) for CPs **3-4**, (NO_2-H_2BDC, dmbpy) for CPs **5-7**, and (CH_3-H_2BDC, dmbpy) for CPs **8-9.** From the structures descriptions above, we can see that the solvent media is crucial in determining the structures of the resultant CPs.

At the solvothermal condition (DMF), CP **1** is obtained without the auxiliary N-donor ligand (dmbpy) within the structure. The same synthetic procedure, well-known MOF-**5** was synthesized when the dmbpy ligand was not added. The μ_3-BDC ligands with mode I link dinuclear zinc units to generate a linear chain of $[Zn_2(BDC)(DMF)_3]_n$, in which the chains are further connected into a (4,4) layered structure through μ_4-BDC ligands (mode II) if the dinuclear zinc units and BDC ligands are regarded as nodes and linkers, respectively. **2** was prepared by the same procedure as described for **1**, only solvent media DMF was replaced by H_2O/EtOH (volume radio 1:1) and shows a wave-like infinite chain built from dmbpy ligands with partly deprotonated BDC ligands (mode III) point alternately up and down. **3** was prepared under solvothermal condition (DMF) and represents a charged anionic MOF with the charge-balancing $[Me_2NH_2]^+$ cations, DMF and water guest molecules in the pores. The completely deprotonated Br-BDC ligand with modes IV-V in **3** links trinuclear zinc clusters to generate a wave-like infinite chain (Scheme 1). The chains are further extended by sharing metal centers to give rise to the 3D framework of **3**

with 5-connected **sqp** topology. During the synthesis of **4**, the solvent media is changed to deionized water and ethanol with volume ratio of 1:1. There exists one dinuclear zinc building block formed by two zinc ions and four μ_4-Br-BDC ligands with mode V (Scheme 1). Then the repeated dinuclear zinc building blocks and Br-BDC ligands connect with each other to generate 2D layer structure with the rigid μ_2-dmbpy struts (Scheme 1, mode VIII) point alternately up and down, which the neighboring layers are further linked to an ideal three-dimensional structure with 6-connected **jsm** topology. CP **5** was prepared by the same procedure as described for **4**, only NO_2-H_2BDC was taken instead of Br-H_2BDC. But unlike to **4**, no dmbpy ligands were found in **5**. The $[Zn_6O_{22}]$ hexanuclear and $[Zn_7O_{24}]$ heptanuclear building blocks of **5** are linked into a 3D framework with 6-connected **pcu** topology based on NO_2-BDC ligands with one coordination mode (Scheme 1, mode V), μ_3-O and μ_2-O atoms. When the solvent media was just changed to deionized water and keep the same reaction conditions, CP **6** involving the NO_2-BDC and dmbpy ligands was obtained. **6** exhibits a 3D framework with (3,4)-connected **dmc** topology which was constructed from μ_3-NO_2-BDC anions and μ_2-dmbpy ligands (Scheme 1: modes VI and VIII). Interestingly, CP **7**, obtained with a H_2O/ACN volume ratio of 1:1, exhibits a 2D (4,4) network based on μ_3-NO_2-BDC anions and a *trans* bidentate bridging dmbpy ligands (Scheme 1, modes VII-VIII). The lattice water molecules and acetonitrile molecules are located in cavities of the **7**, allowing them to participate in O-H⋯O hydrogen bonds with the carboxylate oxygen atoms and aqua ligands, which help to extend the 2D network into a 3D framework. At the outset, the $ZnCl_2 \cdot 6H_2O$ as

the metal ion source was used to prepared of CP **7**. However, the crystals produced were impure and small in size, which can not be characterized by single crystal X-ray diffraction. At the hydrothermal condition (H_2O/EtOH), CP **8** was prepared and shows a 2D (4,4) network constructed by CH_3-BDC ligands with mode I and dmbpy struts with mode VIII (Scheme 1). After the solvent media was just changed to deionized water, a 3D framework with (3,4)-connected **dmc** topological structure based on μ_3-NO_2-BDC anions and μ_2-dmbpy ligands (Scheme 1: modes V and VIII) was prepared (CP **9).**

Based on the discussion above, we come to the conclusion that the structural diversity of CPs **1-9** alters as the organic ligands and solvent media change during synthetic processes.

Thermal and chemical stability. To characterize the CPs in terms of thermal stability, we performed the thermogravimetric analysis (TGA). The relevant experiments for the crystalline samples of CPs **1-9** were performed in a N_2 atmosphere wherein the sample was heated to 800 °C at a rate of 10 °C/min. The TG curves are shown in Fig. S2 and the results reveal that all of nine CPs demonstrate the good thermal stability. CP **1** has three weight loss steps. The first corresponding to the release of one free DMF molecule is observed from 160 °C to 220 °C (calcd. 9.72%, obsd. 9.52%). The second corresponding to the release of one three DMF molecules is observed from 250 °C to 300 °C (calcd. 29.15%, obsd. 29.27%). Then a weight loss occurred above 300 °C due to the decomposition of the structure. CP **2** has thermal stability as no strictly clean weight loss step occurs below 160 °C. The sharp weight

loss above 160 °C corresponds to the decomposition of the framework. For CP **3**, the weight loss in the temperature range of 25-140 °C corresponds to the removal of three DMF and three lattice water molecules (calcd. 17.90%, obsd. 17.72%). Then, it follows a continuous weight loss from 140-170 °C attributed to the release of two $[Me_2NH_2]^+$ cations (calcd. 6.03%, obsd. 5.95%). The compound begins to decompose when the temperature is raised to 380 °C. **4** has thermal stability as no strictly clean weight loss step occurs below 350 °C. Then a sharp weight loss occurred above 350 °C due to the decomposition of the structure. **5** has three weight loss steps. The first corresponding to the release of six free water molecules and one NO_3 anion is observed from 80 °C to 150 °C (calcd. 11.08%, obsd. 11.22%). The second corresponding to the release of two aqua ligands, one μ_3-OH and three μ_2-OH groups is observed from 150°C-200°C (calcd. 6.78%, obsd. 6.92%). The weight-loss step occurred above 400 °C which corresponds to the decomposition of the framework structure. The TGA curve for **6** shows a weight loss near 150 °C, which corresponds to the loss of two aqua ligands (calcd. 4.68%, obsd. 5.01%). Upon further heating, the framework was stable up to 400 °C and then a sharp weight loss was observed above 400 °C due to the collapse of the framework. For **7**, three weight loss steps were observed. The first corresponding to the escape of one lattice water molecule and one acetonitrile molecule is observed from 50 °C -100 °C (calcd. 12.02%, obsd. 12.13%). The second corresponding to the escape of one aqua ligand is observed from 120 °C-150 °C (calcd. 3.67%, obsd. 3.81%). The weight loss step occurred above 380 °C corresponds to the decomposition of framework structure. For **8**, the first refer to the

release of one lattice water molecule is observed from 120-180 °C (calcd. 5.10%, obsd. 5.21%). The sharp weight loss above 350 °C corresponds to the decomposition of the framework. CP **9** has thermal stability as no strictly clean weight loss step occurs below 400 °C. Then a sharp weight loss above 400 °C corresponds to the decomposition of the framework.

The pH-dependent stabilities of **1-9** in aqueous solutions were investigated by XRPD (Fig. S3-S11). For these tests, 50 mg of as-synthesized **1-9** were soaked in aqueous solutions with different pH values and stirred for 3 days at room temperature. According to these results, **1** and **3** are unstable in air, and CPs **2**, **4-9** are stable at pH range from 5 to 9. Stirring under more basic (pH = 13-14) or acidic (pH = 2-3) conditions, CPs **4** and **6-9** show partial decomposition of their frameworks, but CP **2** and **5** show complete decomposition of their framework may be due to the 1D chain structure of **2** is easier to be attacked by water molecules, and without the dmbpy ligands within the framework of **5**, respectively. The stabilities of CPs **4** and **6-9** are similar to several aluminum-isophthalate-based MOFs (CAU-10-X, where X = H, CH_3, OCH_3, NO_2, NH_2, OH),[1d] but lower than the series of carboxylate-based MOFs involving zirconium ions.[18] However, the results is very remarkable, especially when compared with other CPs constructed from aromatic carboxylate, N-containing auxiliary ligands and zinc/cadmium ions.[19]

Luminescent Properties. Luminescent properties of coordination polymers with d^{10} metal centers have attracted intense interest because of their potential applications.[20] Herein, we examined the luminescent properties of the nine CPs in the

solid state at room temperature. As shown in Fig. 10, the photo-luminescent spectra of compounds **1-9** show the emission maxima at 428 nm for **1** (λ_{ex} = 306 nm), 459 nm for **2** (λ_{ex} = 320 nm), 406 nm for **3** (λ_{ex} = 288 nm), 413 nm for **4** (λ_{ex} = 303 nm), 462 nm for **5** (λ_{ex} = 370 nm), 465 nm for **6** (λ_{ex} = 346 nm), 460 nm for **7** (λ_{ex} = 381 nm), 470 nm for **8** (λ_{ex} = 330 nm) and 475 nm for **9** (λ_{ex} = 338 nm), respectively. In comparison to the emission of the free H_2BDC, Br-H_2BDC, NO_2-H_2BDC and CH_3-H_2BDC,[14b,21] The emission maximums of CPs **1-9** have changed and show red-shifts. It is possible that a combination of several factors together,[21c,22] including a change in the highest occupied molecular orbital and lowest unoccupied molecular orbital energy levels of deprotonated BDC^{2-}/ Br-BDC^{2-}/ NO_2-BDC^{2-}/ CH_3-BDC^{2-} anions and neutral ligands (dmbpy) coordinating to metal centers, a charge-transfer transition between ligands and metal centers, and a joint contribution of the intraligand transitions or charge-transfer transitions between the coordinated ligands and the metal centers. However, since the Zn^{II} and Cd^{II} ions are difficult to oxidize or reduce, these bands should also be assigned to the intraligand fluorescent emissions[23] that are tuned by the metal-ligand interactions and deprotonated effect of the dicarboxyl ligands. The maxima emission peaks of **3** and **4** are shorter than other CPs described in this article. It backs the fact up that the electron-withdrawing group and heavy ion of –Br has a positive effect on the quenching of the photoluminescence signal.[24]

Conclusion

Assembly of zinc(II)/cadmium(II) salt with V-shaped linker molecule of substituted

1,3-benzene dicarboxylic acid (H_2BDC/Br-H_2BDC/NO_2-H_2BDC/CH_3-H_2BDC) and methyl-functionalized dmbpy ligand, results in the formation of nine zinc/cadmium-based CPs with a 1D chain, three diverse 2D (4,4) networks, five diverse 3D frameworks of **sqf**, **jsm**, **pcu** and **dmc** topologies, respectively. The pH-dependent stabilities of **1-9** in aqueous solutions were investigated and the results reveal that **2** and **4-9** are stable in aqueous solutions at pH range from 5 to 9. In addition, photoluminescence of the CPs were studied in the solid state at room temperature. The results revealed that both the organic ligands and solvent media play an important role in governing the final structures of **1-9**.

Acknowledgements. This work was supported by the Special Funds of Guangdong College Students' Scientific and Technological Innovation Cultivation (pdjh2015a0562), the Natural Science Foundation of Guangdong Province (2015A030310407), the project of provincial key platform of Guangdong Province (2014KTSPT040), the Distinguished Young Talents in Higher Education of Guangdong Province (2014KQNCX222) and the Natural Science Foundation of Zhaoqing University (201532).

† Electronic Supplementary Information (ESI) available: X-ray crystallographic files (CIF), IR spectra, thermogravimetric curves, PXRD patterns of CPs **1-9.** Table of bond lengths of nine CPs**.** Hydrogen bond geometries for CPs **2** and **6-8.** CCDC: 1433847-1433848, 1415618-1415622, 1433849-1433850.

References

(1) (a) Y. N. Gong, Y. R. Xie, D. C. Zhong, Z. Y. Du, T. B. Lu, *Cryst. Growth Des.* **2015**, 15, 3119; (b) H. Wu, Q. Gong, D. H. Olson, J. Li, *Chem. Rev.* **2012**, 112, 836; (c) T. Kundu, S. C. Sahoo, R. Banerjee, *Cryst. Growth Des.* **2012**, 12, 4633; (d) H. Reinsch, M. A. Veen, B. Gil, B. Marszalek, T. Verbiest, D. Vos, N. Stock, *Chem. Mater.* **2013**, 25, 17; (e) L. Liu, Z. B. Han, S. M. Wang, D. Q. Yuan, S. W. Ng, *Inorg. Chem.*, **2015**, 54, 3719; (f) W. Zhang, R. G. Xiong, *Chem. Rev.* **2012**, 112, 1163; (g) B. Li, Z. Li, R. J. Wei, F. Yu, X. Chen, Y. P. Xie, T. L. Zhang, J. Tao, *Inorg. Chem.*, **2015**, 54, 3331; (h) D. Ma, W. Wang, Y. Li, C. Daiguebonne, G. Calvez, O. Guillou, *CrystEngComm* **2010**, 12, 4372; (i) W. Xie, S. R. Zhang, D. Y. Du, J. S. Qin, S. J. Bao, J. Li, Z. M. Su, W. W. He, Q. Fu, Y. Q. Lan, *Inorg. Chem.*, **2015**, 54, 3290; (j) D. Y. Ma, Z. Li, J. X. Xiao, R. Deng, P. F. Lin, R. Q. Chen, Y. Q. Liang, H. F. Guo, B. Liu, J. Q. Liu, *Inorg. Chem.* **2015**, 54, 6719; (k) Y. Hu, Z. Liu, J. Xu, Y. Huang, Y. Song, *J. Am. Chem. Soc.* **2013**, 135, 9287.

(2) (a) A. S. Rao, A. Pal, R. Ghosh, S. K. Das, *Inorg. Chem.* **2009**, 48, 1802; (b) L. Liu, S. P. Huang, G. D. Yang, H. Zhang, X. L. Wang, Z. Y. Fu, J. G. Dai, *Cryst. Growth Des.* **2010**, 10, 930.

(3) (a) X. Wan, F. Jiang, L. Chen, M. Wu, M. Zhang, J. Pan, K. Su, Y. Yang, M. Hong, *Cryst. Grwoth Des.* **2015**, 15, 1481; (b) H. Liu, Y. Zhao, Z. Zhang, N. Nijem, Y. J. Chabal, H. Zeng, J. Li, *Adv. Funct. Mater.* **2011**, 21, 4754; (c) C. P. Li, M. Du, *Chem. Commun.* **2011**, 47, 5958; (d) M. Eddaoudi, J. Kim, N. Rosi, D. Vodak, J. Wachter, M. O'Keeffe, O. M. Yaghi, *Science* **2002**, 295, 469.

(4) (a) D. Ma, Y. Li, Z. Li, *Chem. Commun.* **2011**, 47, 7377; (b) J. Canivet, A. Fateeva, Y. Guo, B. Coasne, D. Farrusseng, *Chem. Soc. Rev.* **2014**, 43, 5594; (c) J.W. Zhang, C.C. Zhao, Y.P. Zhao, H.Q. Xu, Z.Y. Du, H.L. Jiang, *CrystEngComm* **2014**, 16, 6635; (d) S.S. Kaye, A. Dailly, O.M. Yaghi, J.R. Long, *J. Am. Chem. Soc.* **2007**, 129, 14176; (e) J. Yang, A. Grzech, F.M. Mulder, T.J. Dingemans, *Chem. Commun.* **2011**, 47, 5244.

(5) (a) S M. Kandiah, M.H. Nilsen, S. Usseglio, S. Jakobsen, U. Olsbye, M. Tiset, C. Larabi, E.A. Quadrelli, F. Bonino, K.P. Lillerud, *Chem. Mater.* **2010**, 22, 6632; (b) H. Li, W. Shi, K. Zhao, H. Li, Y. Bing, P. Cheng, *Inorg. Chem.* **2012**, 51, 9200; (c) H. Jasuja, K.S. Walton, *Dalton Trans.* **2013**, 42, 15421.

(6) (a) H. Liu, Y. Zhao, Z. Zhang, N. Nijem, Y. J. Chabal, X. Peng, H. Zeng, J. Li, *Chem. Asian J.* **2013**, 8, 778; (b) D. Y. Ma, X. Li, X. G. Wu, X. Q. Chen, Z. R. Xu, F. D. Liu, D. F. Huang, H. F. Guo, *J. Mol. Struct.* **2015**, 1083, 421.

(7) (a) Bruker. APEXII software, Version 6.3.1, Bruker AXS Inc, Madison, Wisconsin, USA (**2004**); (b) G. M. Sheldrick, *Acta Cryst.* **2008**, A64, 112; (c) Spek, A. L. *PLATON, A Multipurpose Crystallographic Tool*; Utrecht University: Utrecht, The Netherlands, **2005**.

(8) (a) V. A. Blatov, A. P. Shevchenko, D. M. Proserpio, *Cryst. Groweh Des.* **2014**, 14, 3576; (b) G. Nandi, R. Thakuria, H. M. Titi, R. Patra, I. Goldberg, *CrystEngComm* **2014**, 16, 5244.

(9) (a) D. B. Dell'Amico, D. Boschi, F. Calderazzo, L. Labella, F. Marchetti, *Inorg. Chim. Acta* **2002**, 330, 149; (b) D. A. Brown, N. J. Fitzpatrick, H. Muller-Bunz, A.

T. Ryan, *Inorg. Chem.* **2006**, 45, 4497.

(10) (a) O. R. Evans, W. Lin, *Chem. Mater.* **2001**, 13, 2705; (b) G. Li, Z. Li, H. Hou, X. Meng, Y. Fan, W. Chen, *J. Mol. Struct.* **2004**, 694, 179; (c) D. Y. Ma, K. Lu, L. Qin, H. F. Guo, X. Y. Peng, J. Q. Liu, *Inorg. Chim. Acta* **2013**, 396, 84.

(11) (a) C. Y. Niu, X. F. Zheng, Y. He, Z. Q. Feng, C. H. Kou, *CrystEngComm* **2010**, 12, 2847; (b) A. Karmakar, R. J. Sarma, J. B. Baruah, *Inorg. Chem. Commun.* **2006**, 9, 1169.

(12) (a) X. Hao, X. Wang, Z. Su, K. Shao, Y. Zhao, Y. Lan, Y. Fu, *Dalton Trans.* **2009**, 40, 8562; (b) X. Wang, Y. Zhang, X. Cheng, X. Chen, *CrysEngComm* **2008**, 10, 753; (c) Y. Tan, Y. He, J. Zhang, *Chem. Commun.* **2011**, 47, 10647; (d) B. Yuan, D. Ma, X. Wang, Z. Li, Y. Li, H. Liu, D. He, *Chem. Commun.* **2012**, 48, 1135.

(13) (a) D. Y. Ma, G. H. Deng, *Acta Cryst.* **2008**, C64, m271; (b) J. Zhang, S. Gao, Z. M. Che, *Eur. J. Inorg. Chem.* **2004**, 956; (c) D. Y. Ma, H. F. Guo, L. Qin, *Chinese J. Struct. Chem.* **2013**, 32, 1229.

(14) (a) Y. H. He, Y. L. Feng, Y. Z. Lan, Y. H. Wen, *Cryst. Growth Des.* **2008**, 8, 3586; (b) X. Lu, J. Ye, W. Li, W. Gong, L. Yang, Y. Lin, G. Ning, *CrystEngComm* **2012**, 14, 1337.

(15) (a) L. Li, B. B. Guo, G. Li, *Inorg. Chem. Commun.* **2013**, 35, 351; (b) A. Sarkar, V. Bertolasi, D. Ray, *Polyhedron* **2012**, 44, 113. (c) W. Q. Kan, J. Yang, Y. Y. Liu, J. F. Ma, *CrystEngComm* **2012**, 14, 6271.

(16) (a) S. C. Manna, E. Zangrando, J. Ribas, N. R. Chaudhuri, *Eur. J. Inorg. Chem.* **2008**, 1400; (b) C. Ma, C. Chen, Q. Liu, F. Chen, D. Liao, L. Li, L. Sun, *Eur. J.*

Inorg. Chem. **2004**, 3316.

(17) (a) N. Lalioti, C. P. Raptopoulou, A. Terzis, A. E. Aliev, I. P. Gerothanassis, E. Manessi-Zoupa, S. P. Perlepes, *Angew. Chem. Int. Ed. Engl.* **2001**, 40, 3211; (b) P. Kanoo, A. C. Ghosh, S. T. Cyriac, T. K. Maji, *Chem.-Eur. J.* **2012**, 18, 237.

(18) A. Schaate, P. Roy, A. Godt, J. Lippke, F. Waltz, M. Wiebcke, P. Behrens, *Chem. Eur. J.* **2011**, 17, 6643.

(19) (a) K. Tan, N. Nijem, Y. Gao, S. Zuluaga, J. Li, T. Thonhauser, Y. J. Chabal, *CrystEngComm* **2015**, 17, 247; (b) B. Chen, C. Liang, J. Yang, D. S. Contreras, Y. L. Clancy, E. B. Lobkovsky, O. M. Dai, S.Yaghi, *Angew. Chem. Int. Ed.* **2006**, 45, 1390.

(20) (a) H. Li, M. Eddaoudi, T. L. Groy, O. M. Yaghi, *J. Am. Chem. Soc.* **1998**, 120, 8571; (b) C. Yue, C. Yan, R. Feng, M. Wu, L. Chen, F. Jiang, M. Hong, *Inorg. Chem.* **2009**, 48, 2873; (c) X. G. Yang, L. R. Jia, S. M. Fang, *Synth. React. Inorg. Met. Org. Nano-Met. Chem.* **2013**, 43, 325; (d) B. Gole, A. K. Bar, P. S. Mukherjee, *Chem. Commun.* **2011**, 47, 12137; (e) A. Barbieri, G. Accorsi, N. Armaroli, *Chem. Commun.* **2008**, 48, 2185; (f) J. An, C. M. Shade, D. A. Chengelis-Czegan, S. Petoud, N. L. Rosi, *J. Am. Chem. Soc.* **2011**, 133, 1220.

(21) (a) L. Zhang, Y.Y. Qin, Z.J. Li, Q.P. Lin, J.K. Cheng, J. Zhang, Y.G. Yao, Inorg. Chem. 2008, 47, 8286; (b) K. K. Bisht, Y. Rachuri, B. Parmar, E. Suresh, *RSC. Adv.* **2014**, 4, 7352 ; (c) K. Jiang, L.F. Ma, X.Y. Sun, L.Y. Wang, *CrystEngComm* **2011**, 13, 330.

(22) S.L. Li, Y.Q. Lan, J.F. Ma, J. Yang, G.H. Wei, L.P. Zhang, Z.M. Su, *Cryst.*

Growth Des. **2008**, 8, 675; (b) S.L. Li, Y.Q. Lan, J.F. Ma, Y.M. Fu, J. Yang, G.J. Ping, J. Liu, Z.M. Su, *Cryst. Growth Des.* **2008**, 8, 1610.

(23) (a) Y. Su, S.Q. Zang, Y.Z. Li, H.Z. Zhu, Q.J. Meng, *Cryst. Growth Des.* **2007**, 7, 1277; (b) L.L. Wen, D.B. Dang, C.Y. Duan, Y.Z. Li, Z.F. Tian, Q.J. Meng, *Inorg. Chem.* **2005**, 44, 7161.

(24) H. R. Wang, H. Guo, *Synth. React. Inorg. Met. Org. Nano-Met. Chem.* **2014**, 44, 974.

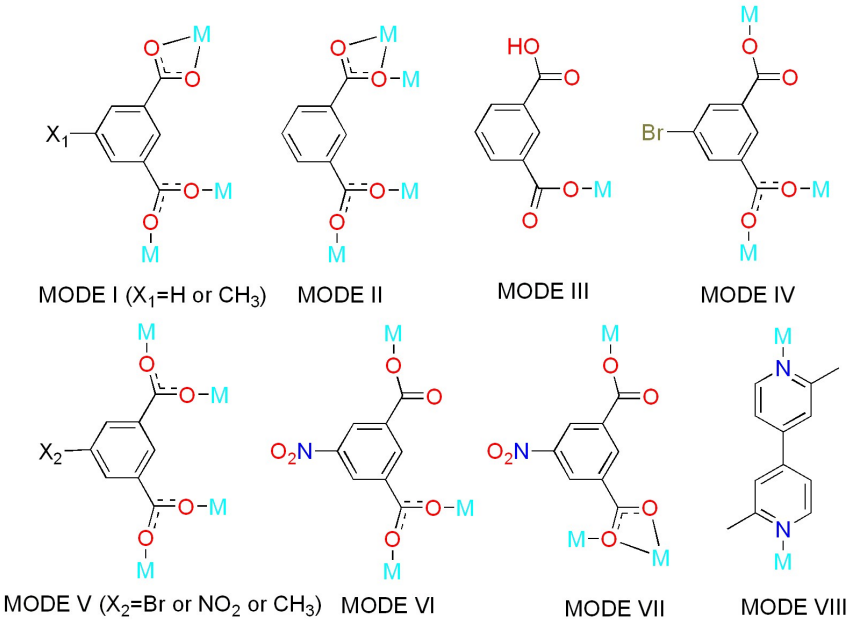

Scheme 1. The coordination modes of X-H_2BDC (X = H, Br, NO_2 and CH_3) ligands in CPs **1-9**.

Table 1 Crystallographic data of complexes **1-9**

	1	**2**	**3**	**4**	**5**
Empirical formula	$C_{28}H_{36}N_4O_{12}Zn_2$	$C_{28}H_{22}N_2O_8Zn$	$C_{45}H_{51}N_5Br_4O_{20}Zn_3$	$C_{28}H_{18}Br_2N_2O_8Zn_2$	$C_{64}H_{40}N_8O_{60}Zn_{13}$
Formula weight	751.35	579.85	1497.66	801.00	2926.93
Temperature (K)	296(2)	293(2)	291(2)	293(2)	291(2)
Size (mm)	0.22×0.20×0.18	0.32×0.28×0.23	0.28×0.24×0.22	0.45×0.30×0.05	0.26×0.22×0.20
Crystal system	monoclinic	triclinic	orthorhombic	orthorhombic	triclinic
Space group	*P21*	*C2c*	*Pbca*	*C2221*	*P-1*
a (Å)	9.919(6)	20.941(4)	20.9786(18)	14.0217(2)	12.8821(14)
b (Å)	16.851(10)	8.9021(18)	24.834(2)	31.3444(5)	14.2922(12)
c (Å)	10.145(6)	15.065(3)	25.206(2)	27.9952(4)	16.9364(17)
α (°)	90.00	90.00	90.00	90.00	110.255(3)
β (°)	93.180(11)	117.91(3)	90.00	90.00	99.167(2)
γ (°)	90.00	90.00	90.00	90.00	106.390(3)
V ($Å^3$)	1693.1(17)	2481.7(8)	13132(2)	12303.9(3)	2689.7(5)
Z	2	4	8	16	1
D ($Mg.m^3$)	1.474	1.552	1.515	1.730	1.807
Limiting indices	$-11 \le h \le 11$, $-18 \le k \le 20$, $-11 \le l \le 12$	$-24 \le h \le 24$, $-10 \le k \le 10$, $-16 \le l \le 18$	$-26 \le h \le 26$, $-31 \le k \le 31$, $-32 \le l \le 32$	$-17 \le h \le 14$, $-38 \le k \le 38$, $-34 \le l \le 34$	$-15 \le h \le 16$, $-18 \le k \le 18$, $-16 \le l \le 21$
Reflections collected/unique	10484/3613	9564/1934	142255/14328	53715/12287	20022/11667
R_{int}	0.0802	0.0433	0.0476	0.0805	0.0790
F(000)	776	1192	5968	6304	1452
θ (°)	2.06-25.20	3.06-25.20	1.64-27.00	3.16-73.95	1.337-26.997
Goodness-of-fit on F^2	0.977	1.063	1.064	1.137	1.059
$R(I>2\sigma)$	R_1 = 0.0651 wR_2 = 0.1509	R_1 = 0.0402 wR_2 = 0.1043	R_1 = 0.0477 wR_2 = 0.1417	R_1 = 0.1373 wR_2 = 0.3158	R_1 = 0.0539 wR_2 = 0.1317
R (all data)	R_1 = 0.1087 wR_2 = 0.1771	R_1 = 0.0447 wR_2 = 0.1081	R_1 = 0.0914 wR_2 = 0.1458	R_1 = 0.1382 wR_2 = 0.3162	R_1 = 0.1038 wR_2 = 0.1616
Largest diff. peak and hole ($Å^{-3}$)	0.76, -0.91	0.74, -0.53	0.62, -0.65	1.01, -0.72	0.99, -1.44

	6	**7**	**8**	**9**
Empirical formula	$C_{28}H_{22}N_4O_{14}Zn_2$	$C_{16}H_{16}N_3O_8Cd$	$C_{15}H_{14}NO_5Zn$	$C_{15}H_{11}NO_4Zn$
Formula weight	769.24	490.72	353.64	334.64
Temperature (K)	293(2)	296(2)	296(2)	293(2)
Size (mm)	0.33×0.27×0.21	0.34×0.28×0.22	0.22×0.20×0.18	0.22×0.20×0.18
Crystal system	monoclinic	triclinic	triclinic	tetragonal
Space group	*P21/c*	*P-1*	*P-1*	I4122
a (Å)	12.5013(5)	8.5151(6)	8.2249(16)	9.946(4)
b (Å)	14.5412(5)	10.0658(7)	9.8672(19)	9.946(4)
c (Å)	8.2241(3)	11.9929(8)	11.221(2)	31.544(13)
α (°)	90.00	67.113(2)	68.441(3)	90.00
β (°)	104.8493(9)	88.027(2)	68.947(4)	90.00
γ (°)	90.00	76.771(2)	66.741(3)	90.00
V ($Å^3$)	1445.08(9)	920.16(11)	753.3(2)	3120(2)
Z	2	2	2	8
D ($Mg.m^3$)	1.768	1.771	1.652	1.587
Limiting indices	$-13 \le h \le 14$, $-16 \le k \le 17$, $-9 \le l \le 7$	$-10 \le h \le 10$, $-7 \le k \le 12$, $-14 \le l \le 14$	$-8 \le h \le 9$, $-10 \le k \le 11$, $-11 \le l \le 13$	$-11 \le h \le 11$, $-11 \le k \le 11$, $-23 \le l \le 37$
Reflections collected/unique	9133/2591	5974/3280	4422/2353	9767/1266
R_{int}	0.0141	0.0169	0.0237	0.0548
$F(000)$	780	490	362	1360
θ (°)	1.69-25.19	1.85-25.16	2.02-25.18	2.15-25.19
Goodness-of-fit on F^2	1.058	1.060	1.090	1.070
$R(I>2\sigma)$	R_1 = 0.0206 wR_2 = 0.0609	R_1 = 0.0257 wR_2 = 0.0651	R_1 = 0.0536 wR_2 = 0.1546	R_1 = 0.0282 wR_2 = 0.0631
R (all data)	R_1 = 0.0219 wR_2 = 0.0618	R_1 = 0.0276 wR_2 = 0.0638	R_1 = 0.0616 wR_2 = 0.1654	R_1 = 0.0359 wR_2 = 0.0678
Largest diff. peak and hole ($Å^{-3}$)	0.35, -0.35	0.81, -0.35	0.96, -0.59	0.26, -0.28

$$R = \sum(\| F_o | - | F_c \|)/\sum | F_o | .$$

$$wR = [\sum w(F_o^2 - F_c^2)^2/\sum w(F_o)^2]^{1/2}.$$

Figure Captions:

Figure 1. (a) The coordination environment for Zn(II) ion in **1**. (b) View of an infinite chain of **1**. (c) View of the 2D (4,4) network of **1**. All H atoms are omitted for clarity in (a)-(c). Symmetry codes: i = x, y, 1+z; ii = 1-x, 0.5+y, -z.

Figure 2. (a) The coordination environment for Zn(II) ion in **2**. (b) View of wave-like infinite chain of **2**. (c) View of the 3D supramolecular structure formed by hydrogen bonds of **2**. (d) View of O-H⋯O and C-H⋯O hydrogen bonds. All H atoms are omitted for clarity in (a)-(c). Symmetry code: i = -x, y, 0.5-z.

Figure 3. (a) The coordination environment for Zn(II) ion in **3**. (b) View of a wave-like infinite chain of **3**. (c) View of the 2D network with rectangle meshes of **3**. (d) View of the 3D framework of **3**. (d) The **sqp** topological network. All H atoms are omitted for clarity in (a)-(d). Symmetry codes: i = -x, -y, -z; ii = -x, 0.5+y, 0.5-z.

Figure 4. (a) The coordination environment for Zn(II) ion in **4**. (b) View of a zigzag -like infinite chain of **4**. (c) View of the 2D network of **4**. (d) View of the 3D framework of **4**. (e) The **jsm** topological network. All H atoms are omitted for clarity in (a)-(e). Symmetry code: i = -1+x, y, z.

Figure 5. (a) Asymmetric unit in the crystal structure of **5**, excluding lattice water molecules. Ball and stick representation of hexanuclear (b) and heptanuclear (c) building blocks. (d) View of an infinite chain of **5**. (e) View of the 2D network of **5**. (f) View of the 3D framework of **5**. (g) The **pcu** topological network. All H atoms are omitted for clarity in (a)-(f). Symmetry codes: i = -x, 2-y, -z; ii = 1-x, 2-y, -z; iii = -x,

1-y, -z; iv = x, -1+y, z; v = 1+x, y, z; vi = -x, 2-y, 1-z; vii = 1-x, 2-y, 1-z; viii = 1-x, 3-y, 1-z.

Figure 6. (a) The coordination environment for Zn(II) ion in **6**. (b) View of a wave-like infinite chain of **6**. (c) View of the 2D network of **4**. (d) View of the 3D framework of **6**. (e) The **dmc** topological network. All H atoms are omitted for clarity in (a)-(d). Symmetry codes: i = x, 1.5-y, 0.5+z; ii = 1-x, 1-y, 1-z.

Figure 7. (a) The coordination environment for Cd(II) ion in **7**. (b) View of a double chain of **7**. (c) View of the 2D (4,4) network of **7**. (d) View of the 3D framework of **7** formed by O-H···O hydrogen bonds. (e) View of the hydrogen bonds in **5**. All H atoms are omitted for clarity in (a)-(c). Symmetry codes: i = x, 1+y, z; ii = -x, 1-y, 1-z.

Figure 8. (a) The coordination environment for Zn(II) ion in **8**. (b) View of an infinite chain of **8**. (c) View of the 2D (4,4) network of **8**. (d) View of the 3D supramolecular structure formed by hydrogen bonds. (e) View of O-H···O hydrogen bonds. All H atoms are omitted for clarity in (a)-(d). Symmetry codes: i = -x, -y, 2-z, ii = -x, 1-y, 2-z.

Figure 9. (a) The coordination environment for Zn(II) ion in **9**. (b) View of an infinite chain of **9**. (c) View of the 3D framework of **9**. (d) The **jsm** topological network. All H atoms are omitted for clarity in (a)-(c). Symmetry codes: i = 1+y, -1+x, -z; ii = 2-x, -y, z; iii = 1-y, 1-x, -z.

Figure 10. The fluorescent emission spectra of **1-9** in solid state at room temperature.

Figures

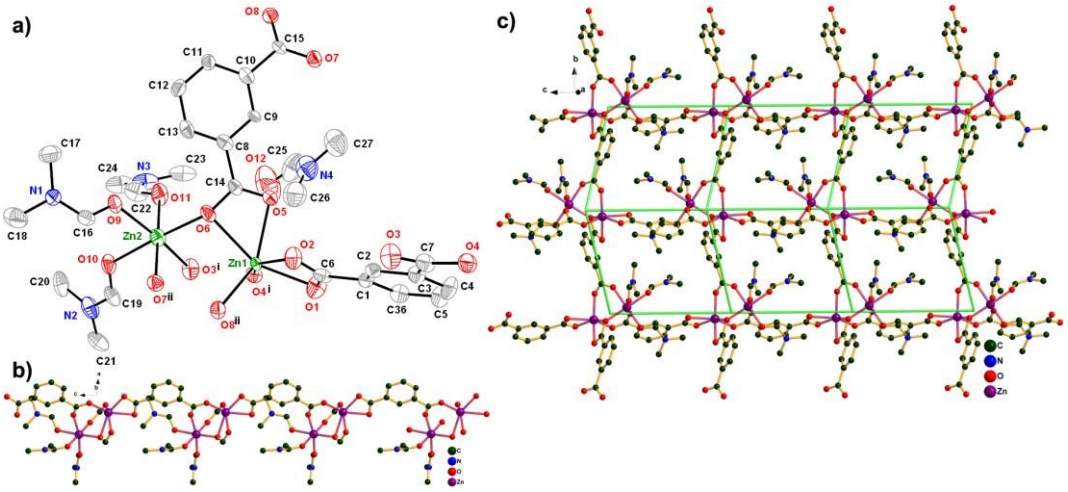

Figure 1. (a) The coordination environment for Zn(II) ion in **1**. (b) View of an infinite chain of **1**. (c) View of the 2D (4,4) network of **1**. All H atoms are omitted for clarity in (a)-(c). Symmetry codes: i = x, y, 1+z; ii = 1-x, 0.5+y, -z.

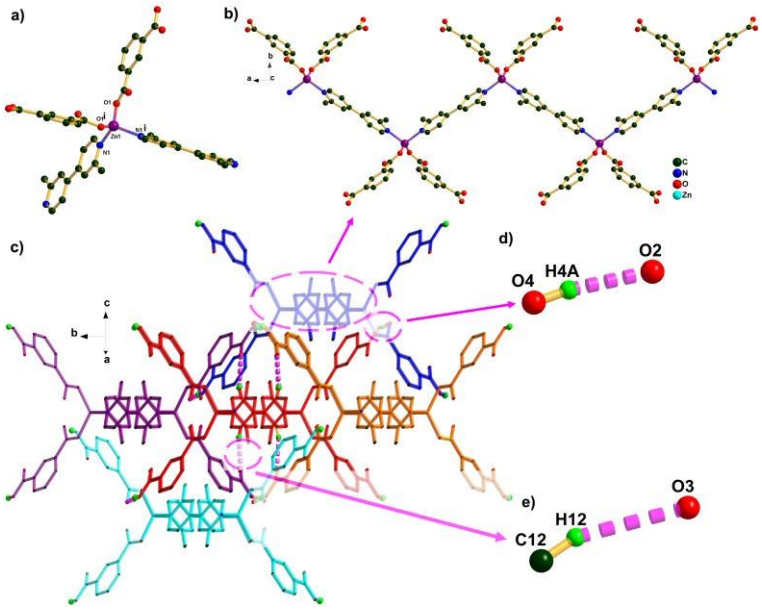

Figure 2. (a) The coordination environment for Zn(II) ion in **2**. (b) View of wave-like infinite chain of **2**. (c) View of the 3D supramolecular structure formed by hydrogen bonds of **2**. (d) View of O-H⋯O and C-H⋯O hydrogen bonds. All H atoms are omitted for clarity in (a)-(c). Symmetry code: i = -x, y, 0.5-z.

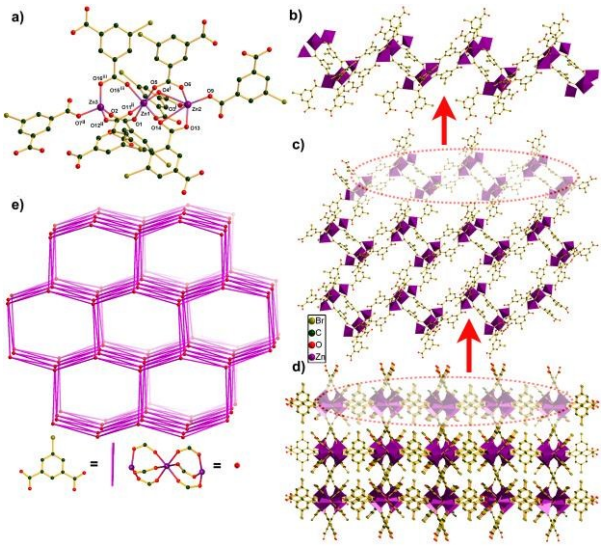

Figure 3. (a) The coordination environment for Zn(II) ion in **3**. (b) View of a wave-like infinite chain of **3**. (c) View of the 2D network with rectangle meshes of **3**. (d) View of the 3D framework of **3**. (d) The **sqp** topological network. All H atoms are omitted for clarity in (a)-(d). Symmetry codes: i = 2-x, 1-y, 2-z; ii = x, 0.5-y, 0.5+z; iii = 0.5+x, 0.5-y, 2-z.

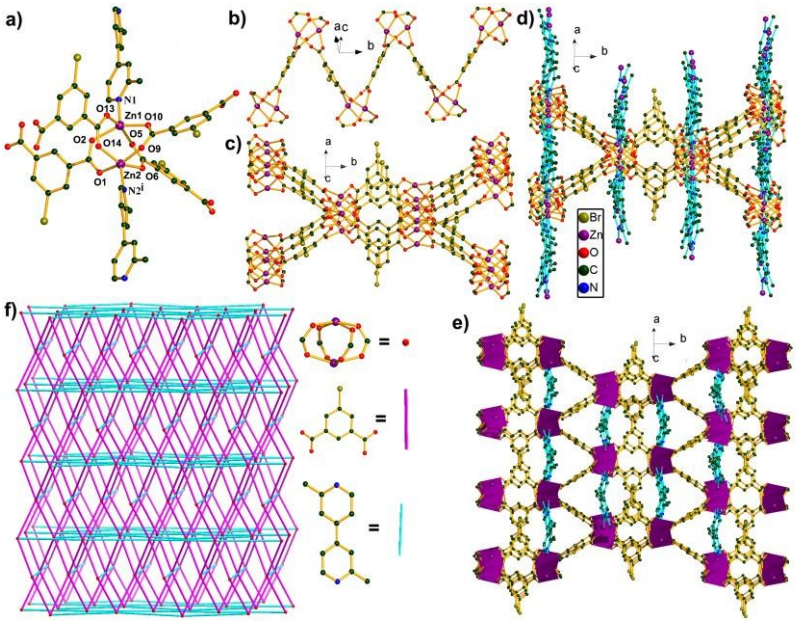

Figure 4. (a) The coordination environment for Zn(II) ion in **4**. (b) View of a zigzag -like infinite chain of **4**. (c) View of the 2D network of **4**. (d) View of the 3D framework of **4**. (d) The **jsm** topological network. All H atoms are omitted for clarity in (a)-(e). Symmetry code: i = -1+x, y, z.

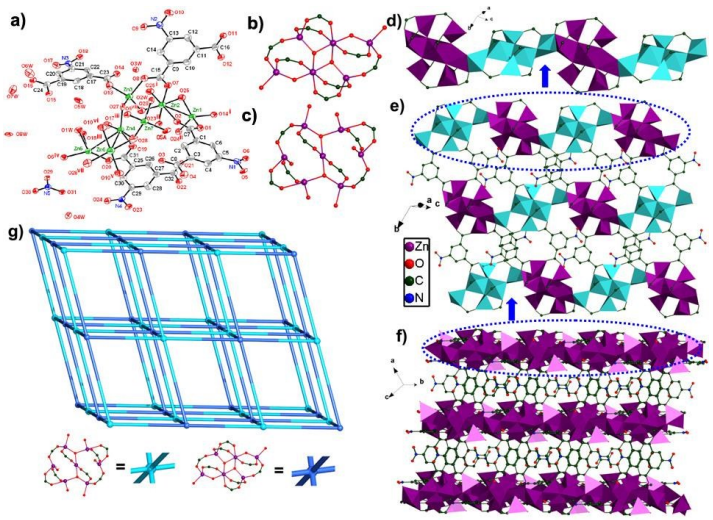

Figure 5. (a) Asymmetric unit in the crystal structure of **5**, excluding lattice water molecules. Ball and stick representation of hexanuclear (b) and heptanuclear (c) building blocks. (d) View of an infinite chain of **5**. (e) View of the 2D network of **5**. (f) View of the 3D framework of **5**. (f) The **pcu** topological network. All H atoms are omitted for clarity in (a)-(f). Symmetry codes: i = -x, 2-y, -z; ii = 1-x, 2-y, -z; iii = -x, 1-y, -z; iv = x, -1+y, z; v = 1+x, y, z; vi = -x, 2-y, 1-z; vii = 1-x, 2-y, 1-z; viii = 1-x, 3-y, 1-z.

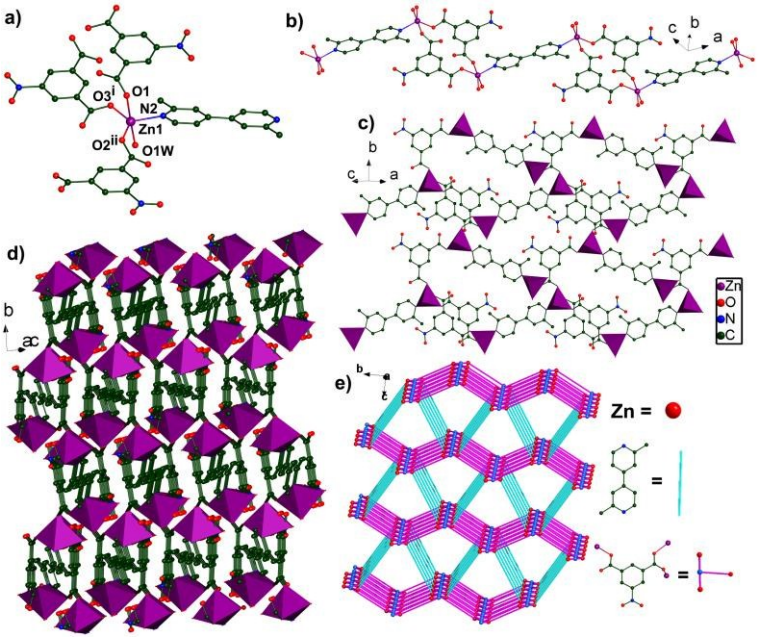

Figure 6. (a) The coordination environment for Zn(II) ion in **6**. (b) View of a wave-like infinite chain of **6**. (c) View of the 2D network of **6**. (d) View of the 3D framework of **6**. (e) The **dmc** topological network. All H atoms are omitted for clarity in (a)-(d). Symmetry codes: i = x, 1.5-y, 0.5+z; ii = 1-x, 1-y, 1-z.

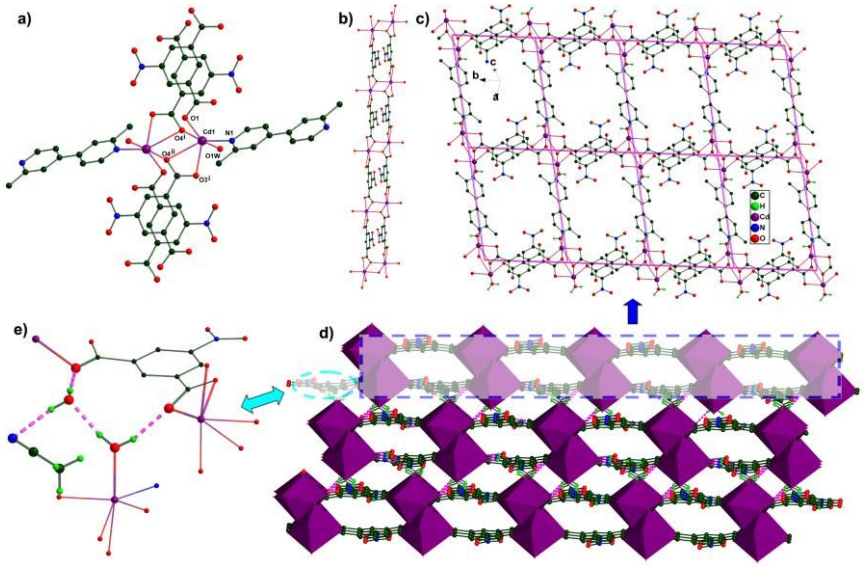

Figure 7. (a) The coordination environment for Cd(II) ion in **7**. (b) View of a double chain of **7**. (c) View of the 2D (4,4) network of **7**. (d) View of the 3D framework of **7** formed by O-H⋯O hydrogen bonds. (e) View of the hydrogen bonds in **7**. All H atoms are omitted for clarity in (a)-(c). Symmetry codes: i = x, 1+y, z; ii = -x, 1-y, 1-z.

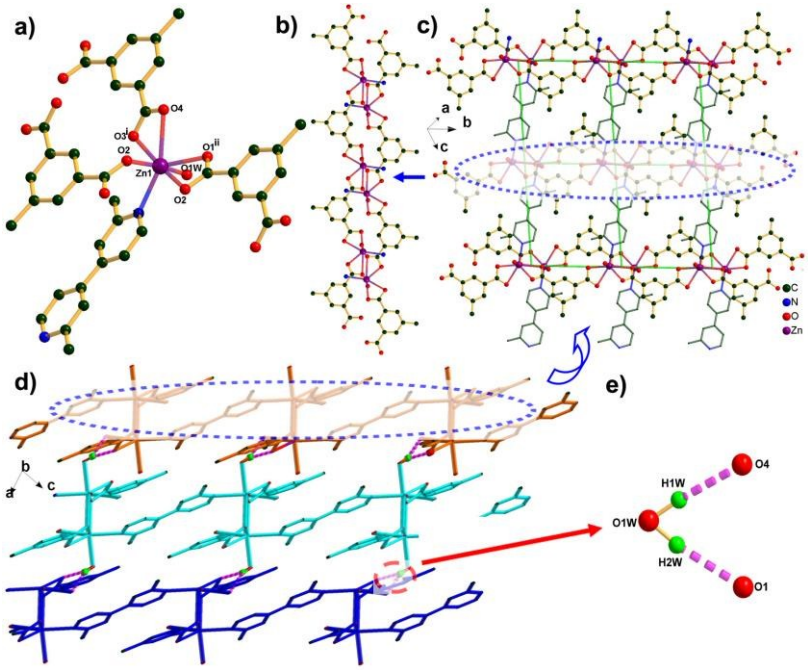

Figure 8. (a) The coordination environment for Zn(II) ion in **8**. (b) View of an infinite chain of **8**. (c) View of the 2D (4,4) network of **8**. (d) View of the 3D supramolecular structure formed by hydrogen bonds. (e) View of O-H⋯O hydrogen bonds. All H atoms are omitted for clarity in (a)-(d). Symmetry codes: i = -x, -y, 2-z, ii = -x, 1-y, 2-z.

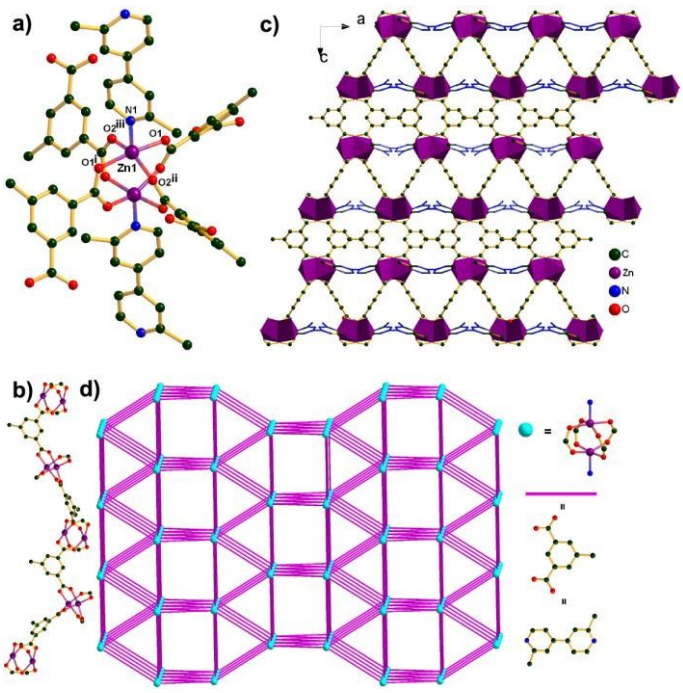

Figure 9. (a) The coordination environment for Zn(II) ion in **9**. (b) View of an infinite chain of **9**. (c) View of the 3D framework of **9**. (d) The **jsm** topological network. All H atoms are omitted for clarity in (a)-(c). Symmetry codes: i = 1+y, -1+x, -z; ii = 2-x, -y, z; iii = 1-y, 1-x, -z.

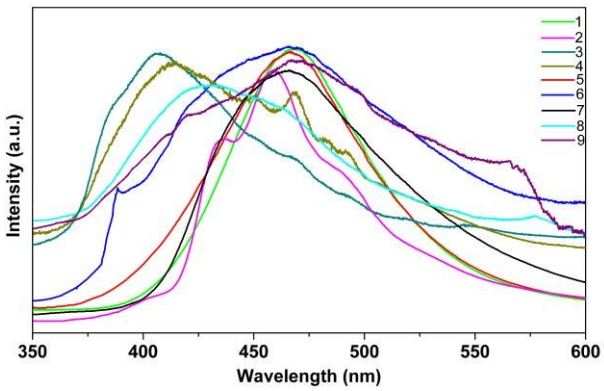

Figure 10. The fluorescent emission spectra of **1**-**9** in solid state at room temperature.